JFM RAPIDS
journals.cambridge.org/rapids

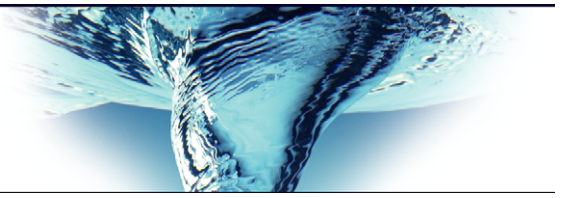

Lagrangian accelerations of particles in superfluid turbulence

M. La Mantia†, D. Duda, M. Rotter and L. Skrbek

Faculty of Mathematics and Physics, Charles University, Ke Karlovu 3, 121 16 Prague, Czech Republic

(Received 26 November 2012; revised 2 January 2013; accepted 10 January 2013; first published online 7 February 2013)

Quantum turbulence in thermal counterflow of superfluid ^{4}He is studied at length scales comparable to the mean distance ℓ between quantized vortices. The Lagrangian dynamics of solid deuterium particles, of radius R_p about one order of magnitude smaller than ℓ, is analysed in a planar section of the experimental volume by using the particle tracking velocimetry technique. We show that the average amplitude of the acceleration of the particles seems to increase as the temperature decreases and applied heat flux increases and this can be explained by exploiting the two-fluid model of superfluid ^{4}He. We also report that, at the probed length scales, the normalized distribution of the acceleration of the particles appears to follow an unexpected classical-like behaviour.

Key words: particle/fluid flow, quantum fluids, vortex dynamics

1. Introduction

Turbulence, which occurs in many different natural systems, represents an open and challenging problem of modern physics. It spans an enormous range of length scales, from the size of galaxies, of the order of 10^{20} m, down to the size of the core of quantized vortices in superfluid ^{4}He, of the order of 10^{-10} m. Quantized vortices are the consequence of the fundamental quantum mechanical restriction on the circulation of the superfluid velocity, which cannot be arbitrary, as in classical viscous fluids, but is equal to an integer multiple of the quantum of circulation $\kappa = h/m$, where h is the Planck constant and m denotes the atomic mass of ^{4}He. The dynamical behaviour of a tangle of quantized vortices is an essential ingredient of quantum turbulence (QT), which can loosely be defined as the most general form of motion of fluids displaying superfluidity. At finite temperature, the gas of thermal excitations can be considered as a viscous fluid and superfluid ^{4}He, also called He II, displays the two-fluid behaviour. Two velocity fields exist, one in the viscous normal fluid, which carries the entire entropy content of He II, the other in the inviscid superfluid. In the

† Email address for correspondence: lamantia@nbox.troja.mff.cuni.cz

doi:10.1017/jfm.2013.31

presence of quantized vortices the two flow fields are coupled via the mutual friction force and both can be turbulent, as shown by Guo *et al.* (2010). QT in He II at finite temperature (above ∼1 K) is therefore physically even richer than classical turbulence and represents a challenging field of research combining low-temperature physics and fluid dynamics; see, for example, the reviews by Vinen & Niemela (2002) and Skrbek & Sreenivasan (2012) for further details on QT.

Modern visualization methods utilizing small particles that follow the flow, such as particle image velocimetry (PIV) and particle tracking velocimetry (PTV), have contributed in an essential way to recent progress in classical fluid mechanics. These techniques have already been used at low temperatures and led, e.g., to the direct visualization of quantized vortices in He II (Bewley, Lathrop & Sreenivasan 2006), even though their application is difficult for both technical (optical access to the cryogenic experimental volume, choice of suitable particles) and fundamental reasons (existence of two velocity fields, interaction of particles with quantized vortices); see, for example, the reviews by Sergeev & Barenghi (2009) and Van Sciver & Barenghi (2010) for further details on the implementation of flow visualization techniques at low temperatures.

Important results have recently been obtained by using such techniques in one particular quantum flow of He II, called thermal counterflow, which has no equivalent in classical fluid dynamics. Thermal counterflow can be easily set up in He II by applying a voltage to a resistor (heater) located at the closed end of a flow channel, open to a helium bath at the other end. Assuming that the heat flux q applied at the heater is used to convert the approaching superfluid into normal fluid, the average velocity of the outgoing normal fluid is $V_n = q/\rho ST$, where T denotes the temperature, S represents the temperature-dependent specific entropy of He II (that is, of its normal component, as the superfluid component does not carry entropy) and its – approximately constant – total density ρ is the sum of the temperature-dependent densities of its normal, ρ_n, and superfluid, ρ_s, components. In this way a relative (counterflow) velocity V_{ns} is created along the channel, which can be easily evaluated from the condition of conservation of mass. Upon exceeding relatively small values of V_{ns}, which is proportional to the applied heat flux, the heat transport is affected by QT due to the appearance of a tangle of quantized vortices. Its intensity is represented by the vortex line density L, the total length of vortex lines in a unit volume. The visualization results obtained in thermal counterflow of He II include the observation of vortical structures around a cylinder (Zhang & Van Sciver 2005), discovery of non-Gaussian velocity statistics (Paoletti *et al.* 2008) and interesting findings on the trapping mechanisms of particles into the cores of quantized vortices (Chagovets & Van Sciver 2011).

In comparison with classical fluid dynamics, however, the implementation of modern visualization methods to study quantum flows is in its infancy, sometimes posing more questions than giving clear answers. For example, the trapping mechanism of particles into the cores of quantized vortices deserve further attention and study. There is a clear need for more detailed analyses by flow visualization, which is being proven as a valuable tool to study cryogenic flows. A step forward is to focus on Lagrangian accelerations in quantum flows. This research field is indeed well established in classical fluid mechanics and has led to significant progress in understanding turbulent flows, shedding light, e.g., on the longstanding problem of turbulent intermittency (Mordant *et al.* 2001; Voth *et al.* 2002) and on the properties of particle-laden flows (Qureshi *et al.* 2007, 2008; Toschi & Bodenschatz 2009). As quantum flows consist of normal and superfluid velocity fields and might in analogy be thought of as vortex-

laden, it seems natural to expect that acceleration studies will bring new insights in understanding QT in general.

This work represents the first study of accelerations in cryogenic flows. Let us stress that the micrometre-sized particles (much larger than the core of quantized vortices) used are smaller than the mean distance between quantized vortices and thus are capable of probing QT in superfluid ^{4}He directly at length scales where classical and quantum flows are expected to be fundamentally different. We show that in thermal counterflow of He II the observed acceleration statistics can be explained by modelling the interaction between particles and quantized vortices. The ratio of the viscous drag force (acting on the particles in the velocity field of the normal fluid) to the pressure gradient force (attracting the particles to quantized vortices in the superfluid velocity field) seems indeed to display the same temperature and velocity dependence as the average magnitude of the observed accelerations. We also report that, at the probed length scales, the normalized distribution of the acceleration of the particles appears to follow an unexpected classical-like behaviour. The quantum nature of thermal counterflow is therefore not evident from the normalized distribution of the acceleration but its signature is apparent from the temperature and velocity dependence of the acceleration statistics, in the range of investigated parameters.

2. Experimental apparatus and protocol

In order to perform such a study, a novel experimental apparatus for cryogenic flow visualization has been devised, as detailed by La Mantia *et al.* (2012). In short, a low-loss custom-built cryostat is equipped with 25 mm diameter windows enabling optical access to the experimental volume, of square cross-section (sides of 50 mm) and ∼300 mm long. The seeding system supplies micrometre-sized solid deuterium particles, obtained by mixing at room temperature deuterium and helium gases (the ratio between the corresponding moles of ^{4}He and D_2 is typically 100) and injecting the mixture into the helium bath (deuterium solidifies at ∼19 K). A continuous-wave solid-state laser and suitable lenses are used to obtain a laser sheet of less than 1 mm thickness and height of ∼10 mm. A 1 MP digital camera is situated perpendicularly to the laser sheet and its CMOS sensor focused on a 13 mm wide and 8.2 mm high field of view by using an appropriate macro lens. Such a setup enables us to use the PTV technique for measurements of Lagrangian quantities in a plane parallel to the vertical counterflow direction, in the middle of the experimental volume, i.e. as far as possible from its boundaries.

The thermal counterflow is generated by a flat square heater of sides slightly smaller than 50 mm, placed on the bottom of the experimental volume. Once liquid helium is transferred into the cryostat, a pumping unit is used to lower its temperature. The gaseous mixture is then injected, usually at $T \simeq 2.2$ K, and the helium bath stabilized at a chosen temperature. As the particles are not neutrally buoyant (the density of solid D_2 is ∼1.4 times that of liquid ^{4}He), images are recorded before switching on the heater, in order to estimate their settling velocities and dimensions. The heater is then switched on, images collected at different heat fluxes, at 50 f.p.s., and the particle tracks calculated by using an open-source algorithm (Sbalzarini & Koumoutsakos 2005). The corresponding particle velocities and accelerations in the horizontal and vertical directions are estimated by purpose-made computer codes, developed by us; for further details see La Mantia *et al.* (2012).

Several movies were recorded at different temperatures and heat fluxes (each movie is typically made up of 1000 images) and the Lagrangian quantities calculated from

movies obtained under the same conditions were then combined, as shown below. On each image there are typically up to 100 μm sized particles and several thousand trajectories were computed (tracks with up to few hundred points were calculated). The trajectories obtained from the just mentioned tracking algorithm were filtered by using a purpose-made computer program in order to remove spurious, unphysical trajectories before calculating velocities and accelerations. The latter were computed as follows. Once the particle positions were obtained, the velocities along the tracks were calculated by taking into account three consecutive positions, e.g. in the horizontal direction, x_1, x_2 and x_3, and the corresponding time intervals, t_1 and t_2. The horizontal velocity at the intermediate position was then estimated as $[(x_2-x_1)/t_1+(x_3-x_2)/t_2]/2$ (the corresponding vertical velocity was similarly computed). This of course did not apply to the first and last points of the trajectories (two positions were used in these cases). A similar procedure was employed for the accelerations, which were calculated by taking into account three consecutive velocities. Note that this computational approach is simpler than those employed for the Lagrangian analyses of classical turbulent flows, see e.g. Voth *et al.* (2002) and Mordant, Crawford & Bodenschatz (2004*a*). However, as shown below, the calculated particle velocities and accelerations appear to be consistent with the proposed physical description of the problem, at least qualitatively.

3. Results and discussion

The probability density function (p.d.f.) of the particle instantaneous vertical acceleration a_z is displayed in figure 1 as a percentage of the total number of points of the tracks having at least five points, at a constant value of applied heat flux q (figure 1*a*) and temperature T (figure 1*b*). It is evident that the tails of the distributions become wider as T decreases and q increases (the same was observed for the instantaneous horizontal acceleration a_x). Owing to the symmetry of the vertical counterflow, it is natural to assume that the accelerations in horizontal planes are statistically equal. An average acceleration amplitude A can then be defined as the mean of the instantaneous acceleration $(2a_x^2+a_z^2)^{0.5}$. A also increases as T decreases and q increases, see the insets of figure 1.

The data sets shown in figure 1 collapse if the ratio between the acceleration a_z and its standard deviation a_z^{sd} is used for the comparison, see figure 2.

The normalized distribution of the acceleration of the particles can be approximated by the same stretched exponential fit as employed for a turbulent flow in water, at a Taylor-based Reynolds number $Re_\lambda = 690$, i.e.

$$\text{p.d.f.}\,(a) = C\exp\left[\frac{-a^2}{(1+|a\beta/\sigma|^\gamma)\sigma^2}\right], \tag{3.1}$$

where $a = a_z/a_z^{sd}$ and the p.d.f. is expressed as a percentage of the total number of points; $\beta = 0.513$, $\sigma = 0.563$ and $\gamma = 1.600$ (Mordant *et al.* 2004*a*). The constant $C = 21.990$ is 30 times larger than that employed by Mordant *et al.* (2004*a*), where the p.d.f. is normalized differently. Using similar values of the four parameters of (3.1), obtained at $Re_\lambda = 970$ (La Porta *et al.* 2001; Voth *et al.* 2002; Mordant *et al.* 2004*a*), does not appreciably alter the statement that the observed acceleration follows a classical-like behaviour, at the probed length scales.

The same outcome is obtained if another fit, associated with a log-normal distribution of the acceleration magnitude of classical turbulent flows

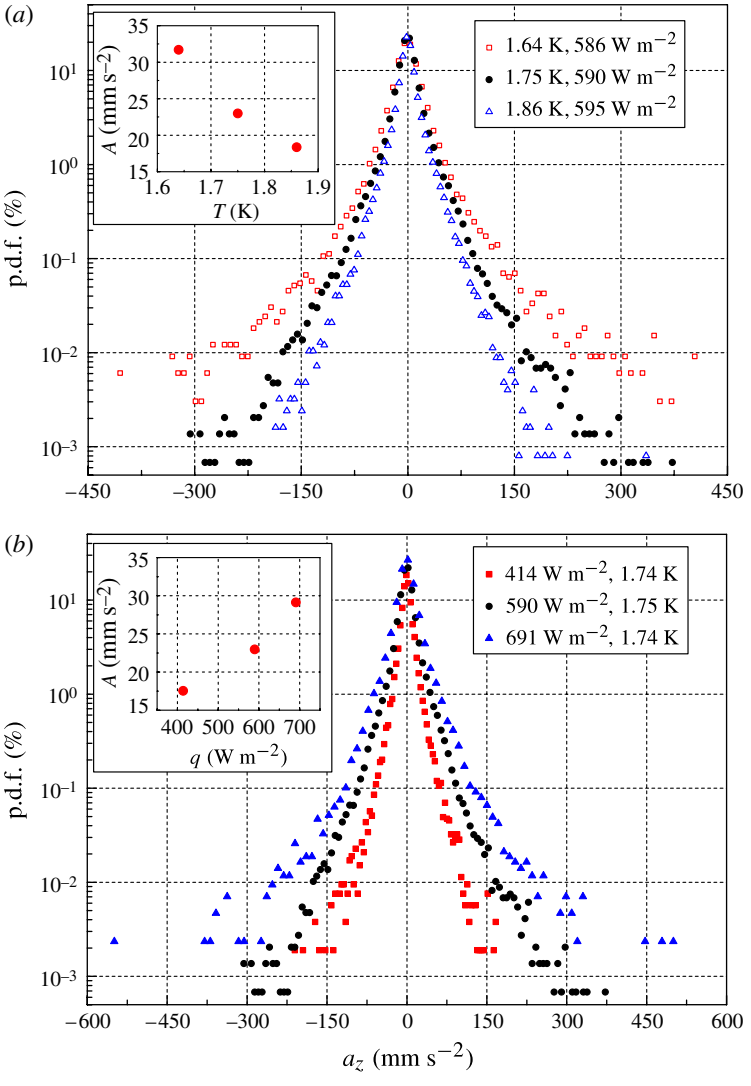

FIGURE 1. p.d.f. of the instantaneous vertical acceleration a_z, shown as a percentage of the total number of points of the trajectories having at least five points, for (*a*) constant applied heat flux q and (*b*) constant temperature T. Red squares: 1.74 K, 414 W m^{-2}, 52 327 points and 1514 tracks; open red squares: 1.64 K, 586 W m^{-2}, 32 861 points and 1355 tracks; black circles: 1.75 K, 590 W m^{-2}, 146 586 points and 4419 tracks; open blue triangles: 1.86 K, 595 W m^{-2}, 124 579 points and 3065 tracks; blue triangles: 1.74 K, 691 W m^{-2}, 42 612 points and 1744 tracks. (*a*) Inset: average acceleration amplitude A as a function of T at constant q; (*b*) inset: A as a function of q at constant T.

(Mordant *et al.* 2004*b*; Qureshi *et al.* 2007, 2008), is used for the comparison, i.e.

$$\text{p.d.f.}\,(a) = \frac{N\exp(3s^2/2)}{4\sqrt{3}}\left[1 - \text{erf}\left(\frac{\ln|a/\sqrt{3}| + 2s^2}{\sqrt{2}s}\right)\right], \tag{3.2}$$

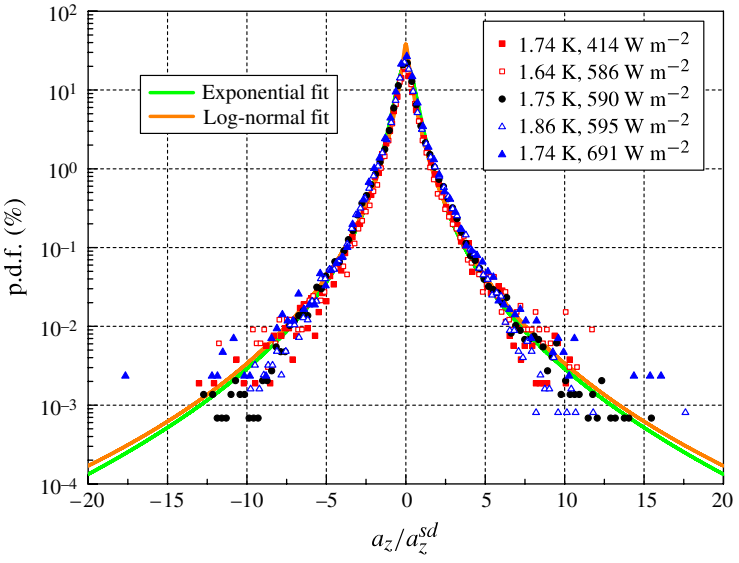

FIGURE 2. p.d.f. of a_z/a_z^{sd}, where a_z^{sd} is the standard deviation of a_z. Symbols as in figure 1; green line: exponential fit of the data, (3.1) (Mordant *et al.* 2004*a*); orange line: log-normal fit, (3.2) (Mordant, Crawford & Bodenschatz 2004*b*).

where $s = 1$ (Mordant *et al.* 2004*b*). The constant $N = 30$ is 30 times larger than that employed by Mordant *et al.* (2004*b*), owing to different normalization assumptions. Besides, the flatness of the distributions was estimated to be around 20, even though it could not be accurately calculated, owing to the fact that the current data sets are smaller than those obtained for classical turbulent flows.

This is certainly a novel result, especially in view of the experimentally established fact that the velocities of particles in thermal counterflow seem to have non-classical distributions (Paoletti *et al.* 2008; La Mantia *et al.* 2012). The latter are indeed obtained also in the present case, i.e. the corresponding velocity distributions appear to display a non-Gaussian behaviour, with power-law tails. An example of such a non-classical behaviour is shown in figure 3, for the normalized horizontal velocity of the particles.

The power-law shape of the velocity distribution tails has been linked to vortex reconnections (Paoletti *et al.* 2008), even though it can also be obtained when vortex reconnections do not occur, such as in classical systems of vortex points (White *et al.* 2010). The strongly non-Gaussian form of the velocity distributions might however be seen as a fundamental property of quantum turbulence, supporting the quantum mechanical description of superfluid ^{4}He as a tangle of quantized vortices. It serves as a signature that clearly distinguishes quantum flows from classical turbulent flows, which are usually characterized by nearly Gaussian velocity distributions. A quasi-classical behaviour can indeed be recovered at length scales larger than the average distance ℓ between quantized vortices, as shown numerically by Adachi & Tsubota (2011) and Baggaley & Barenghi (2011).

Our experimental results can be understood in the framework of the following simple theoretical model. The equation of motion for a spherical particle of radius R_p

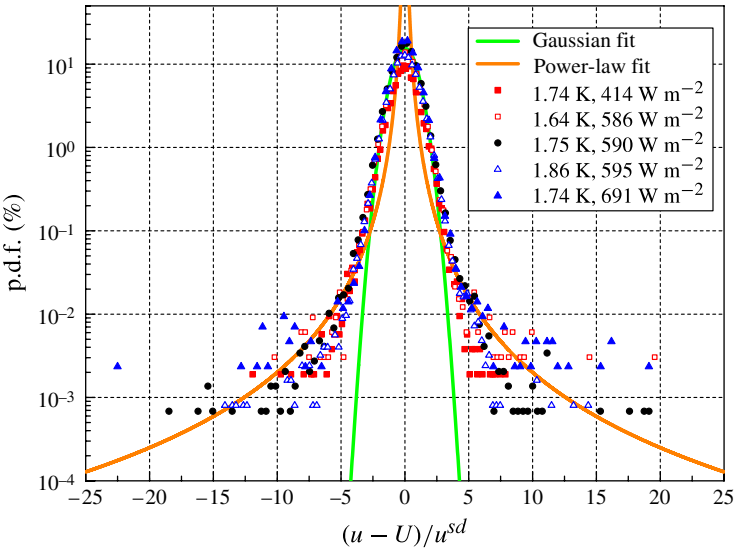

FIGURE 3. p.d.f. of $(u-U)/u^{sd}$, where u is the instantaneous horizontal velocity; U and u^{sd} denote the mean and standard deviation of u, respectively. Symbols as in figure 1; green line: Gaussian fit of the data; orange line: power-law fit $2\,|(u-U)/u^{sd}|^{-3}$.

and density ρ_p in the absence of gravity reads

$$\frac{\mathrm{d}v_p}{\mathrm{d}t} = \frac{9\mu_n}{2\rho_0 R_p^2}(v_n - v_p) + \frac{3\rho_n}{2\rho_0}\frac{\mathrm{D}v_n}{\mathrm{D}t} + \frac{3\rho_s}{2\rho_0}\frac{\mathrm{D}v_s}{\mathrm{D}t}, \tag{3.3}$$

where v_p is the particle velocity, t denotes the time and μ_n is the dynamic viscosity of the normal component of He II; v_n indicates the instantaneous normal fluid velocity, v_s is the instantaneous superfluid velocity and $\rho_0 = \rho_p + \rho/2$; see Poole *et al.* (2005) and Sergeev *et al.* (2007) for further details.

The ratio between the viscous drag force, per unit of mass, acting on the particle, and the pressure gradient force, per unit of mass, attracting the particle to a superfluid vortex core, can be written as

$$\Lambda = \left[\frac{9\mu_n}{2\rho_0 R_p^2}(V_n - v_p)\right] \Big/ \left[\frac{3\rho_s}{2\rho_0}\frac{\kappa^2}{8\pi^2}\nabla\left(\frac{1}{r^2}\right)\right], \tag{3.4}$$

where r denotes the distance between the particle and vortex core. As reported by Sergeev *et al.* (2007), the second term on the right-hand side of (3.3) does not play any significant role when the particle is relatively close to the vortex and thus it has been neglected here. The denominator of Λ has been written as the radial pressure force, per unit of mass, attracting the particle to the vortex core (Sergeev *et al.* 2007). For constant radius R_p of the particle the ratio Λ can be seen as proportional to the parameter

$$\zeta = \mu_n(V_n - v_p)/\rho_s, \tag{3.5}$$

which has dimensions (m^3 s^{-2}). As T decreases (or q increases), ζ increases, similarly to the average acceleration magnitude A, see the insets of figure 1. This can be

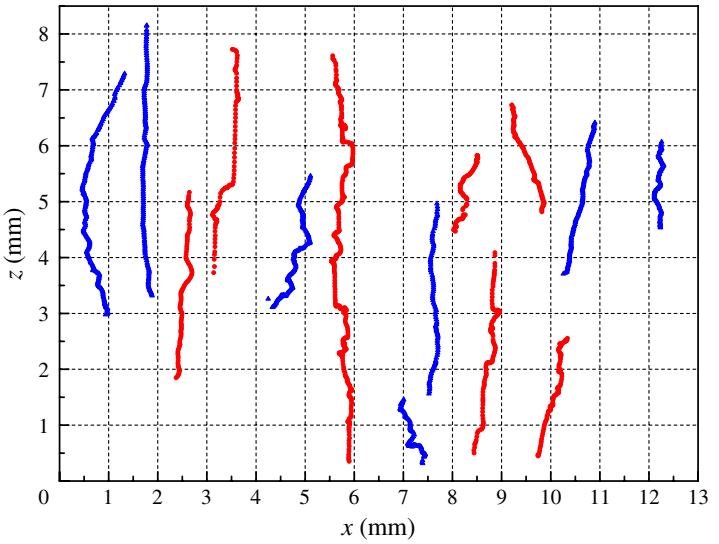

FIGURE 4. Sample trajectories at 1.75 K and 590 W m^{-2} (all shown tracks have at least 100 points; the relative horizontal positions of some of them were changed for the sake of illustration; red circles: tracks of particles moving upwards, as the normal fluid flow; blue triangles: trajectories of particles moving downwards, as the superflow).

	A increases by (%)	ζ increases by (%)
T decreases from 1.86 to 1.75 K	25	25
T decreases from 1.75 to 1.64 K	38	22
T decreases from 1.86 to 1.64 K	73	52

TABLE 1. Temperature T dependence of the average acceleration amplitude A and parameter ζ, at applied heat flux $q \simeq 588$ W m^{-2}, see also figure 1(a).

explained by noting that the particles, as T decreases (or q increases), appear to be less likely to be trapped into the vortices, which can be assumed to be moving at a steady velocity. The pressure gradient force would affect trajectories of the particles, and the corresponding accelerations, without eventually leading to particle trapping (Sergeev *et al.* 2007). This appears to be consistent with the trajectories obtained (some of them are displayed in figure 4) and would also result in the observed increase of A.

The experimental results support, in a qualitative way, such a theoretical picture, see tables 1 and 2. For example, A increases by 25 % when T decreases from 1.86 to 1.75 K, and ζ also increases by 25 %. At constant T, ζ increases by 21 %, when q increases from 590 to 691 W m^{-2}, while A increases by 27 %. These figures were obtained by considering the average v_p of the particle velocities in the vertical direction, that of the imposed counterflow, as calculated from the images. Note however that, when T decreases from 1.75 to 1.64 K, A increases by 38 %, while ζ increases by 22 % (when q increases from 414 to 590 W m^{-2}, ζ increases by 23 %, while A increases by 31 %). This is probably due to the fact that fewer tracks were

	A increases by (%)	ζ increases by (%)
q increases from 414 to 590 W m^{-2}	31	23
q increases from 590 to 691 W m^{-2}	27	21
q increases from 414 to 691 W m^{-2}	66	50

TABLE 2. Applied heat flux q dependence of the average acceleration amplitude A and parameter ζ, at temperature $T \simeq 1.75$ K, see also figure 1(*b*).

obtained at 1.64 K; the same applies to the data at 414 and 691 W m^{-2}, see the caption of figure 1.

Equation (3.3) holds if the particle Reynolds number $Re_p = 2\rho_n R_p(V_n - v_p)/\mu_n$ is lower than 1. In the present case $Re_p \simeq 1$ and this means that (3.3) can only be seen as an approximate model of the observed physical process. Moreover, the particle size distribution, centred on $R_p \simeq 4$ μm and ranging approximately between 2 and 6 μm, could influence the outcome, see (3.4). Note also that not all the particles can be considered spherical and that some of them have been seen rotating (La Mantia *et al.* 2012).

Equation (3.4) is written assuming implicitly that at any time the particle interacts predominantly with one quantized vortex, that is, its interaction with other vortices in the tangle is neglected. Such a treatment requires that the particle is smaller than, or at least comparable to, the mean distance between quantized vortices, which for known vortex line density L can be estimated as $\ell \simeq 1/\sqrt{L}$, see e.g. Skrbek & Sreenivasan (2012). In thermal counterflow the relationship between L and q is known and, in the present case, we estimate ℓ to be between 60 and 100 μm, thus exceeding the mean size of the particles. The average distance travelled by the particles between frames is however of the order of ℓ, the average particle velocity being a few mm s^{-1}, and this means that thermal counterflow is here studied at length scales comparable to ℓ.

The reason why the quantum nature of thermal counterflow does not appear evident from the normalized distributions of the acceleration plotted in figure 2 remains unknown, as at the same probed length scales its quantum signature seems apparent from the velocity distributions, as displayed for example in figure 3, and from the temperature and velocity dependence of the acceleration statistics, as detailed above. Note however that (3.1) and (3.2) appear to be closer to the experimental data in the proximity of the distribution core, similarly to the velocity distributions, which seem to have a Gaussian, classical-like core and power-law tails, see also Paoletti *et al.* (2008) and La Mantia *et al.* (2012). We could therefore argue that in the range of investigated parameters it might be difficult to distinguish between classical-like and quantum behaviour from the acceleration distributions as these may follow similar laws, while the classical and quantum laws obtained for the velocity distributions appear to be significantly different.

4. Conclusions

It has been shown for the first time that in QT – thermal counterflow of ^{4}He – the amplitude of the acceleration of particles seems to increase with decreasing temperature and increasing heat flux. This behaviour can be understood as a relative increase of the viscous drag force, acting on the particles in the velocity field of the normal fluid, compared to the pressure gradient force, attracting the particles to

quantized vortices in the superfluid velocity field. This result, together with the non-classical velocity distributions, might be regarded as a quantum-mechanical signature of thermal counterflow. Additionally, it was shown that, at the probed length scales, the normalized distribution of the acceleration of the particles appears to follow an unexpected classical-like behaviour.

Further investigations are desirable, however, to prove more convincingly the proposed model of the observed physical process, that is, to verify that it holds under different experimental conditions, over broader ranges of heat flux and temperature. Larger data sets should also be collected, at larger frame rates, in order to probe superfluid turbulence at length scales significantly smaller than the average distance between quantized vortices, where classical and quantum flows are expected to be fundamentally different.

Acknowledgements

We thank S. Babuin, C. F. Barenghi, G. P. Bewley, T. V. Chagovets, V. S. L'vov, D. Schmoranzer, Y. A. Sergeev, V. Uruba and J. Vejražka for fruitful discussions and valuable help. We acknowledge the support of GAČR P203/11/0442 and one of us (M. L. M.) also EU COST Action MP0806. We finally thank the anonymous reviewers for their useful suggestions and remarks.

References

Adachi, H. & Tsubota, M. 2011 Numerical study of velocity statistics in steady counterflow quantum turbulence. *Phys. Rev.* B **83**, 132503.

Baggaley, A. W. & Barenghi, C. F. 2011 Quantum turbulent velocity statistics and quasiclassical limit. *Phys. Rev.* E **84**, 067301.

Bewley, G. P., Lathrop, D. P. & Sreenivasan, K. R. 2006 Superfluid helium: visualization of quantized vortices. *Nature* **441**, 588.

Chagovets, T. V. & Van Sciver, S. W. 2011 A study of thermal counterflow using particle tracking velocimetry. *Phys. Fluids* **23**, 107102.

Guo, W., Cahn, S. B., Nikkel, J. A., Vinen, W. F. & McKinsey, D. N. 2010 Visualization study of counterflow in superfluid ^{4}He using metastable helium molecules. *Phys. Rev. Lett.* **105**, 045301.

La Mantia, M., Chagovets, T. V., Rotter, M. & Skrbek, L. 2012 Testing the performance of a cryogenic visualization system on thermal counterflow by using hydrogen and deuterium solid tracers. *Rev. Sci. Instrum.* **83**, 055109.

La Porta, A., Voth, G. A., Crawford, A. M., Alexander, J. & Bodenschatz, E. 2001 Fluid particle accelerations in fully developed turbulence. *Nature* **409**, 1017–1019.

Mordant, N., Crawford, A. M. & Bodenschatz, E. 2004*a* Experimental Lagrangian acceleration probability density function measurement. *Physica* D **193**, 245–251.

Mordant, N., Crawford, A. M. & Bodenschatz, E. 2004*b* Three-dimensional structure of the Lagrangian acceleration in turbulent flows. *Phys. Rev. Lett.* **93**, 214501.

Mordant, N., Metz, P., Michel, O. & Pinton, J.-F. 2001 Measurement of Lagrangian velocity in fully developed turbulence. *Phys. Rev. Lett.* **87**, 214501.

Paoletti, M. S., Fisher, M. E., Sreenivasan, K. R. & Lathrop, D. P. 2008 Velocity statistics distinguish quantum turbulence from classical turbulence. *Phys. Rev. Lett.* **101**, 154501.

Poole, D. R., Barenghi, C. F., Sergeev, Y. A. & Vinen, W. F. 2005 Motion of tracer particles in He II. *Phys. Rev.* B **71**, 064514.

Qureshi, N. M., Arrieta, U., Baudet, C., Cartellier, A., Gagne, Y. & Bourgoin, M. 2008 Acceleration statistics of inertial particles in turbulent flow. *Eur. Phys. J.* B **66**, 531–536.

QURESHI, N. M., BOURGOIN, M., BAUDET, C., CARTELLIER, A. & GAGNE, Y. 2007 Turbulent transport of material particles: an experimental study of finite size effects. *Phys. Rev. Lett.* **99**, 184502.

SBALZARINI, I. F. & KOUMOUTSAKOS, P. 2005 Feature point tracking and trajectory analysis for video imaging in cell biology. *J. Struct. Biol.* **151**, 182–195.

SERGEEV, Y. A. & BARENGHI, C. F. 2009 Particles-vortex interactions and flow visualization in ^{4}He. *J. Low Temp. Phys.* **157**, 429–475.

SERGEEV, Y. A., WANG, S., MENEGUZ, E. & BARENGHI, C. F. 2007 Influence of normal fluid disturbances on interactions of solid particles with quantized vortices. *J. Low Temp. Phys.* **146**, 417–434.

SKRBEK, L. & SREENIVASAN, K. R. 2012 Developed quantum turbulence and its decay. *Phys. Fluids* **24**, 011301.

TOSCHI, F. & BODENSCHATZ, E. 2009 Lagrangian properties of particles in turbulence. *Annu. Rev. Fluid Mech.* **41**, 375–404.

VAN SCIVER, S. W. & BARENGHI, C. F. 2010 Visualisation of quantum turbulence. In *Progress in Low Temperature Physics: Quantum Turbulence* (ed. M. Tsubota & W. P. Halperin), pp. 247–303. Springer.

VINEN, W. F. & NIEMELA, J. J. 2002 Quantum turbulence. *J. Low Temp. Phys.* **128**, 167–231.

VOTH, G. A., LA PORTA, A., CRAWFORD, A. M., ALEXANDER, J. & BODENSCHATZ, E. 2002 Measurement of particle accelerations in fully developed turbulence. *J. Fluid Mech.* **469**, 121–160.

WHITE, A. C., BARENGHI, C. F., PROUKAKIS, N. P., YOUD, A. J. & WACKS, D. H. 2010 Nonclassical velocity statistics in a turbulent atomic Bose–Einstein condensate. *Phys. Rev. Lett.* **104**, 075301.

ZHANG, T. & VAN SCIVER, S. W. 2005 Large-scale turbulent flow around a cylinder in counterflow superfluid ^{4}He (He(II)). *Nat. Phys.* **1**, 36–38.